NUMERICAL SIMULATION OF REFINING ROLLING PROCESS BASED ON ADAPTIVE BEM PARALLEL ALGORITHM

Huancheng Zhang[1,2], Yunhua Qu[1], Aimin Yang[1], Fanqiang Meng[2] and Hongfu Ma[2]

ABSTRACT: First, the paper constructs three-dimensional elastoplastic frictional contact adaptive boundary element method and respectively introduces boundary element space and two solid state of contact, then proposes three-dimensional elastoplastic BEM. Second, the paper constructs two adaptive control technology models. Finally the paper designs parallel condensed algorithm. In the algorithm, we combine with three algorithms and do numerical simulation. So we can reduce the system steady-state error, reduce the system overshoot amount, improve the system response speed and improve calculation accuracy and computational efficiency.

KEY WORDS: Refined rolling; Numerical simulation; Adaptive control technology; BEM; Parallel algorithm

.

.

1 INTRODUCTION

Rolling problems is mainly the study of elastic-plastic contact problem of roller and rolled piece. The calculation precision of rolling force parameters not only depends on the problem solving method for the simulation precision of the original problem, but also depends on the accuracy of the method itself. So choosing a high precision problem solving method for simulating rolling process is very important. In recent years, numerical solution gets rapid development, finite element method is successfully applied in rolling field, and rolling theory and technology have new progress.

The boundary element method is a powerful tool in computational mechanics and computational mathematics. Compared with FEM[1], due to the dimension reduction, construction of BEM discrete grid is relatively simple. However, from the viewpoint of improving computational efficiency and preventing human subjective errors, we still need to develop the method which can automatically generate optimized discrete grid. The basic idea of adaptive boundary element method is to use computer to automatically determine and improve the accuracy of BEM solution. Obviously, the addition of the adaptive process is of great significance.

[1] North China University of Science and Technology, Tangshan 063000, Hebei, China

[2] College of Light Industry, North China University of Science and Technology, Tangshan 063000, Hebei, China

In the paper, the rolling process is seen as united whole of roll and rolling piece and we use frictional contact elastoplastic boundary element method to simulate the rolling process. At the same time the paper studies parallel computing method. Then we use adaptive BEM parallel algorithm to numerically simulate refining rolling process. This avoids the disadvantage of usual practice of splitting rolled piece and roll. So we have achieved good results with the fewest number of assumptions.

2 THREE - DIMENSIONAL ELASTOPLASTIC FRICTIONAL CONTACT ADAPTIVE BEM

2.1. Boundary element space of three-dimensional bem

The boundary element method is a numerical method to solve the boundary integral equation. Contact between two objects occurs on its borders. Proof of existence and uniqueness of BEM solution of frictional contact problem is beginning from boundary element space after solid boundary discretization.

2.1.1. Three-dimensional solid discrete boundary element

We have several methods to get the numerical solution by the discretization of the boundary integral equation[2], for example, on the

engineering calculation using the configuration method or collocation method. No matter what discrete method you use, you need to discrete boundary, including discrete boundary function. The description of the boundary element has two parts: description of boundary element geometry and boundary function interpolation approximate.

Let boundary Γ be surface in three-dimensional space [3]. We construct approximate surface Γ_h of Γ and give geometrical description of boundary element and piecewise interpolation expression of boundary function. Assume Γ is a combination of piecewise smooth closed surface $\Gamma_j (j = 1,2,\cdots,J)$

$$\Gamma = \bigcup_{i=1}^{J} \Gamma_j, \Gamma_i \bigcap \Gamma_j \qquad (1)$$

For each piece surface Γ_j, there is a two sides of single value smooth mapping φ_j, which maps Γ_j to a bounded closed region in the plane. The inverse mapping is $\Phi_j = \varphi_j^{-1}$, so

$$D_j = \varphi_j(\Gamma_j), \Gamma_j = \Phi_j(D_j) \qquad (2)$$

Then, assume D_j is a polygon. Thus we similarly use finite element approximation technique: D_j is covered with regular triangle section T_{hj} and then define interpolation function Φ_{jh} of mapping Φ_j on the each element of subdivision T_{hj}. $\Phi_{jh} : D_j \subset R^2 \to R^3$, then we get a surface Γ_{jh} in space and

$$\Gamma_{jh} = \Phi_{jh}(D_j) \qquad (3)$$

Γ_{jh} is the approximate surface of Γ_j, see Fig. (1). The element on T_{hj} is in the role of mapping Φ_{jh} and then we get element on the Γ_{jh}, that is boundary element:

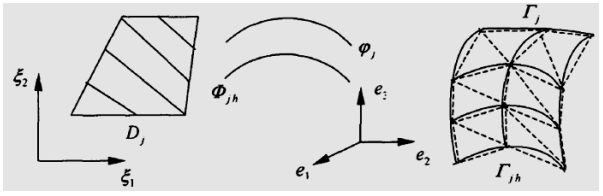

Fig 1. Approximate surface.

2.2. Two solid contact

Contact between solid[4], there are two states in the contact surface: fixed and increase with the increase of external load.

2.2.1. Two solid contact

Define contact area

$$\Gamma_c = \partial\Omega' \bigcap \partial\Omega'' \qquad (4)$$

Decompose $\partial\Omega'$ and $\partial\Omega''$, see Fig. (2).

$$\begin{cases} \partial\Omega' = \Gamma_u \bigcup \Gamma_r' \bigcup \Gamma_k \\ \partial\Omega'' = \Gamma_u \bigcup \Gamma_r'' \bigcup \Gamma_k \end{cases} \qquad (5)$$

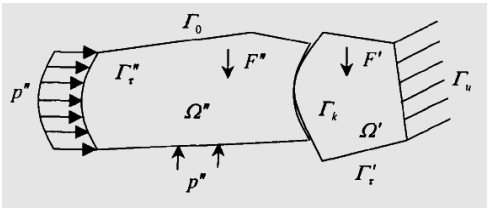

Fig 2. Contact area.

In the Fig. (2), Γ_u, Γ_r', Γ_r'' and Γ_0 are the boundary disjoint part respectively. Assume Γ_u and Γ_k have positive measure. Γ_r', Γ_r'' and Γ_0 have positive measure or zero measure. When contacting, according to the continuous displacement and surface force balance condition, the following relationship has been established on Γ_k

$$\begin{cases} u_n' + u_n'' \le 0 \\ T_n' = T_n'' \le 0 \\ (u_n' + u_n'')T_n' = 0 \\ T_t' = T_t'' = 0 \end{cases} \qquad (6)$$

where $u_n' = u_t' \cdot n_t'$, $u_n'' = u_t'' \cdot n_t''$ and $n' = -n''$.

2.2.1. Increased contact

In the solid deformation process, the contact area may increase[5], see Fig. (3).

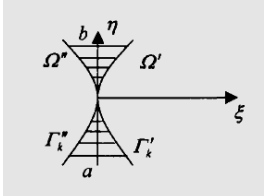

Fig 3. Increased contact area.

Take local coordinate (ξ,η), ξ axis is direction of n'', η axis is tangential direction. Assume

$$\begin{cases}\Gamma_k' = \{(\xi,\eta)|a \le \eta \le b, \xi = f'(\eta)\} \\ \Gamma_k'' = \{(\xi,\eta)|a \le \eta \le b, \xi = f''(\eta)\}\end{cases} \quad (7)$$

where $f'(\eta)$ and $f''(\eta)$ are continuous function on $[a,b]$. So

$$u_\xi'' - u_\xi' \le \varepsilon(\eta), \forall \eta \in [a,b] \quad (8)$$

where $\varepsilon(\eta) = f'(\eta) - f''(\eta)$ is the distance between two objects before deformation, u_ξ'' and u_ξ' are components of the displacement vector in the direction of ξ. So we get

$$\begin{cases}\dfrac{-T_\xi'}{\cos\alpha'} = \dfrac{T_\xi''}{\cos\alpha''} \le 0 \\ T_\eta' = T_\eta'' = 0 \\ (u_\xi'' - u_\xi' - \varepsilon)T_\xi'' = 0\end{cases} \quad (9)$$

$$\begin{cases}\sec\alpha' = \left[1 + \left(\dfrac{df'}{d\eta}\right)^2\right]^{\frac{1}{2}} \\ \sec\alpha'' = \left[1 + \left(\dfrac{df''}{d\eta}\right)^2\right]^{\frac{1}{2}}\end{cases} \quad (10)$$

where α' is the angle between η axis and tangential direction of Γ_k', a'' is the angle between η axis and tangential direction of Γ_k''.

2.3. Three-dimensional elastoplastic bem

For the three-dimensional problem, the fundamental solution of mechanical displacement equation is as follows[6]:

$$u_{ij}^*(p,q) = \frac{1}{16\pi G(1-\nu)}\left[(3-4\nu)\delta_{ij} + r_{,i}r_{,j}\right] \quad (11)$$

$$t_{ij}^*(p,q) = \frac{-1}{8\pi(1-\nu)r^2}\left\{\frac{\partial r}{\partial n}\left[(1-2\nu)\delta_{ij} + 3r_{,i}r_{,j}\right] - (1-2\nu)(r_{,i}n_j - r_{,j}n_i)\right\} \quad (12)$$

where r is the distance from source to field point, $r_{,i}$ is partial derivative of coordinate i, n is normal direction of boundary. Assume boundary of elastomer is divided into M boundary unit and each boundary unit has L nodes. After the discrete processing of boundary integral equation we get

$$c_{ij}u_j(p) = \sum_{m=1}^{M}\sum_{l=1}^{L}\left(\int_{S^e{}_m} N_l^{(L)}(\xi,\eta)u_{ij}^*(\xi,\eta,p)J(\xi,\eta)dS^e(\xi,\eta)\right)t_j(q_l^{(m)}) - \sum_{m=1}^{M}\sum_{l=1}^{L}\left(\int_{S^e{}_m} N_l^{(L)}(\xi,\eta)u_{ij}^*(\xi,\eta,p)J(\xi,\eta)dS^e(\xi,\eta)\right)u_j(q_l^{(m)}) \quad (13)$$

where $t_j(q_l^{(m)})$ is surface force value of m unit's l node and $u_j(q_l^{(m)})$ is component of displacement value along the j direction. We use Gauss integral to deal with the integral of formula (13) and get

$$\int_{S^e{}_m} N_l^{(L)}(\xi,\eta)u_{ij}^*(\xi,\eta,p)J(\xi,\eta)dS^e(\xi,\eta) \approx \sum_{\alpha=1}^{G1}\sum_{\beta=2}^{G2} N_l^{(L)}(\xi_\alpha,\eta_\beta)u_{ij}^*(\xi_\alpha,\eta_\beta,p)J(\xi_\alpha,\eta_\beta)w_\alpha w_\beta \quad (14)$$

$$\int_{S^e{}_m} N_l^{(L)}(\xi,\eta)t_{ij}^*(\xi,\eta,p)J(\xi,\eta)dS^e(\xi,\eta) \approx \sum_{\alpha=1}^{G1}\sum_{\beta=2}^{G2} N_l^{(L)}(\xi_\alpha,\eta_\beta)t_{ij}^*(\xi_\alpha,\eta_\beta,p)J(\xi_\alpha,\eta_\beta)w_\alpha w_\beta \quad (15)$$

where $G1$ and $G2$ are respectively Gauss integral points' number of two directions. Thus, after numerical integration, we obtain system equation set[7]:

$$HU = GT \quad (16)$$

where U and T are respectively node displacement vector and cell surface force vector, H and G are coefficient matrix. Next we rearrange equation. We move unknown quantity to equation left and known quantity to equation right. At the same time we multiply known quantity and the right coefficient matrix. Then we get

$$AX = F \quad (17)$$

where A is coefficient matrix associated with unknown quantity and is an asymmetric full matrix, X is unknown column vector and F is column vector after multiplying known quantity and the right coefficient matrix. We solve equations (11-17) and then get all unknown quantities on the boundary.

2.4. Adaptive control technology computing method

Calculation of adaptive model coefficient has two cases: calculation of current rolled steel coil coefficient and calculation of archived model coefficient. The two calculation methods are the following[8]:

Adaptive coefficient of current rolled steel coil (B'):

$$B' = \frac{P_A}{P_C} \quad (18)$$

where P_A is the actual parameter (for example rolling force) and P_C is setting calculation parameter.

$$C^{'} = (1-K)\cdot C_1 + K\cdot C_B \qquad (19)$$

where K is experiment constant coefficient, C_1 is Historical accumulation coefficient and C_B is current calculation coefficient.

In the high speed rolling process, adaptive model is not a very stable process and there will be certain speed fluctuation and elastoplastic change. So in the adaptive control, how to effectively control the change under high speed steady state is the key process of strip rolling.

2.4.1. Control the change under high speed steady state

Considering the importance of the model parameters and its direct impact on product quality, in the adaptive process, computer judges the speed of strip rolling process and develop principle of carrying out adaptive calculation at the maximum speed. So it can better reduce the errors and defects of rolling process[9]. See Fig. (4).

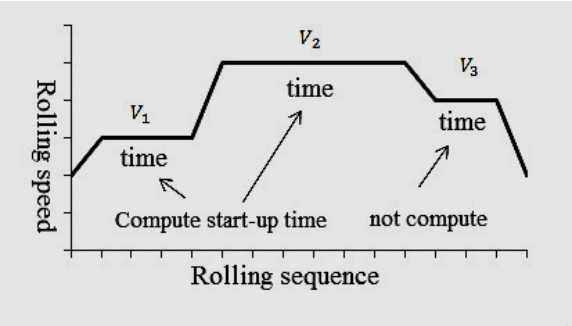

Fig 4. Adaptive calculation in the strip rolling process.

The logic of judgment is $V = Max\{V_1, V_2 \cdots V_t\}$. We take the maximum speed value under every steady state in the strip rolling process: $V_j \geq V$.

Then we compare the current steady state speed with the maximum speed. If the current steady state speed is more than maximum speed, we start the adaptive calculation; Otherwise, the calculation does not start. So we can obtain the best data under steady state.

2.5 Parallel condensation algorithm design

The paper uses a master-slave programming mode[10]. Control program in the programming mode is called primary process. Control program is responsible for the generation of process, initialization, collection and output results. The rest is from process, performing the actual calculation. Each microcomputer is equipped with a from process and primary process is only on one of the microcomputer. Solving a problem is by the primary process and from process. Generation, management of process, communication between each other such as parallel process are realized through calling the PVM library function. Master-slave programming model is suitable for coarse-grained parallel computing. So in the design algorithm, the division of parallel granularity can not too be thin and try to overlap communication and computation.

In the contact problem of rolled piece and roll, contact area accounts for only a small portion of the entire roll system. The condensation process of reserving contact area influence coefficient occupies 80% of the total serial algorithm computing time. And the condensation process of coefficient matrix of roll and rolling piece are successively completed independently. It has a strong parallelism. In order to solve this contradiction, we developed a parallel condensation algorithm: after first forming roll coefficient matrix, it starts the from process to condense; at the same time in the primary process it forms the coefficient matrix of rolled piece and condenses; finally it returns the condensed result of coefficient matrix of the roll through the network and calculates displacement and stress and outputs the result. Programming ideas and processes of master-slave see Fig. (5).

3 NUMERICAL SIMULATION

Because of the symmetry, we see the quarter of rolled piece as a numerical model, see Fig. (6). The input data and calculation conditions see Table 1. In the beginning, the state of rolling process is not stable. When the materials pass the gap between two rolls for rolling, state begins to become stable. Because of the elastic-plastic deformation, we need to calculate domain integral of rolled piece. We divide rolled piece into four hundred eighty eight-node units, see Fig. (7). For the contact problem, we divide working roll into six hundred twenty-eight four-node boundary elements [12].

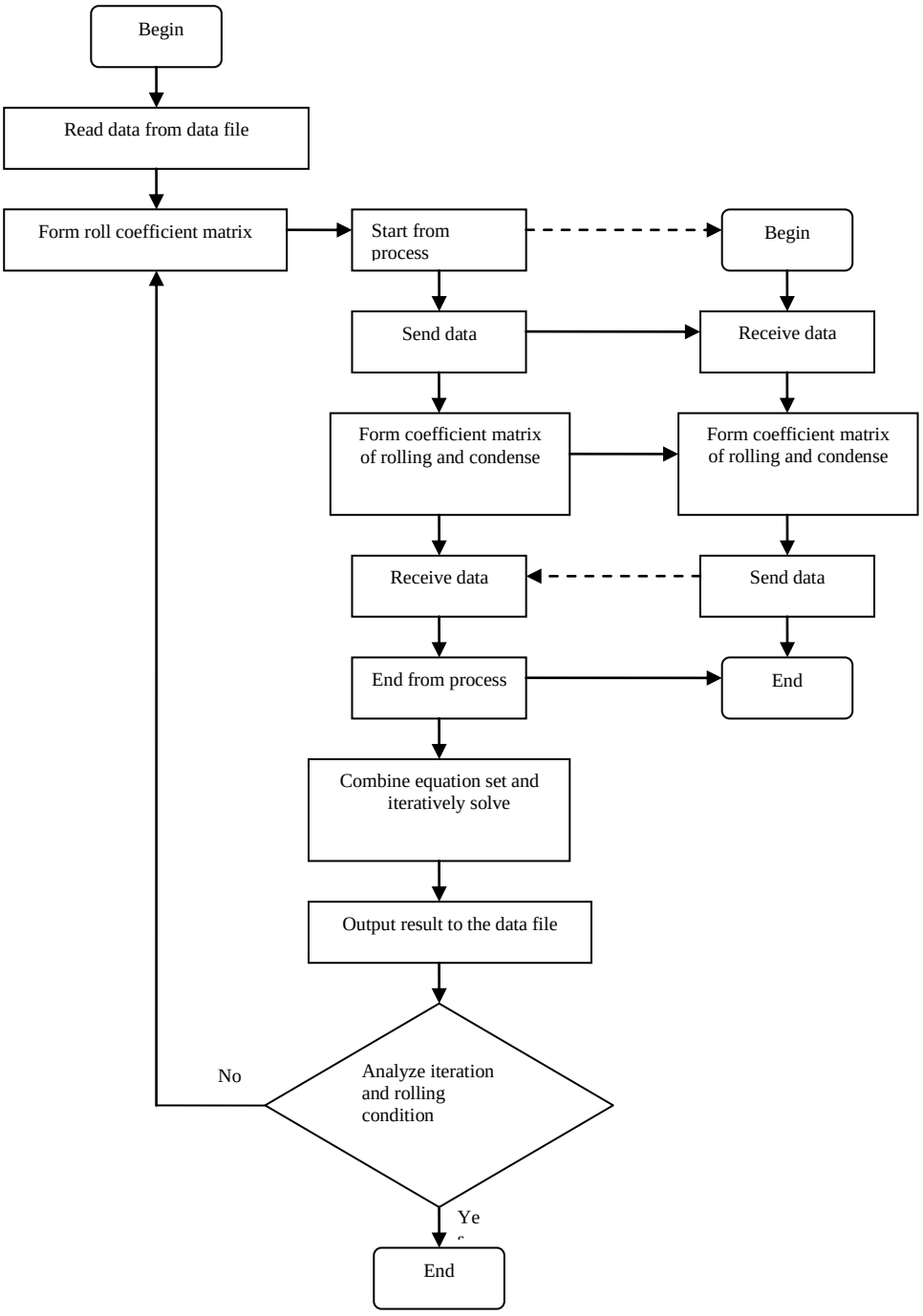

Fig 5. Parallel condensed algorithmic process.

Table 1. Rolling parameter table.

Roll			Strip		
Young modulus	E/GPa	210	Young modulus	E/GPa	150
Poisson ratio	v	0.3	Poisson ratio	v	0.3
Roll radius	R/mm	150	Yield stress	e_s/MPa	280
Length of roll	L/mm	128	Maximum shear stress	k/MPa	162
Initial roll gap	h_1/mm	1.35	Thickness	h_0/mm	1.5
Coulomb friction coefficient		0.008	Hardening coefficient	H	0.001
Shear friction coefficient	m	0.5	Plate width	b/mm	120

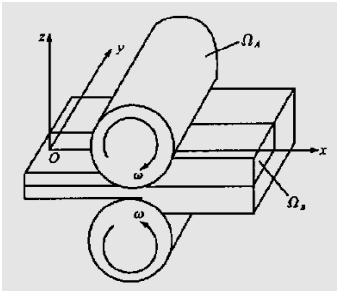

Fig 6. Strip rolling.

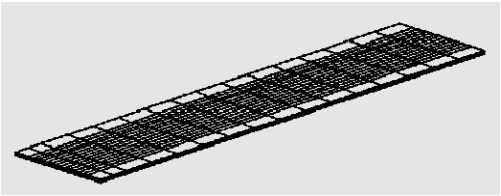

Fig 7. Rolling element.

In two computers connected with Ethernet, we use the parallel algorithm to get the calculation result, see Fig. (8)-(11). The Fig. (8) is rolling pressure distribution between roll and rolling piece and the maximum is 900MPa and the contact area length of strip center is 4.2mm. The Fig. (9) is friction stress distribution on the direction of rolling. The Fig. (10) is friction stress distribution on the direction of plate width. From Fig. (11), due to the elastic deformation of roll, the maximum rolling pressure occurs near the edge.

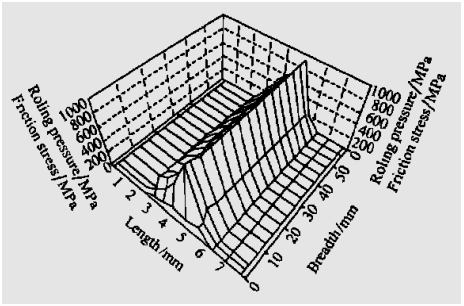

Fig 8. Rolling force distribution.

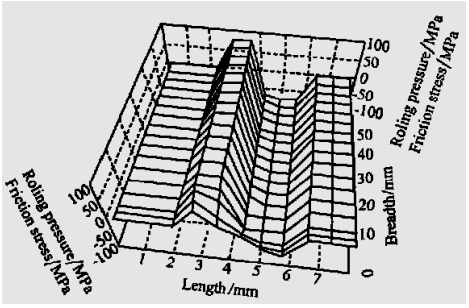

Fig 9. Friction stress distribution along the rolling direction.

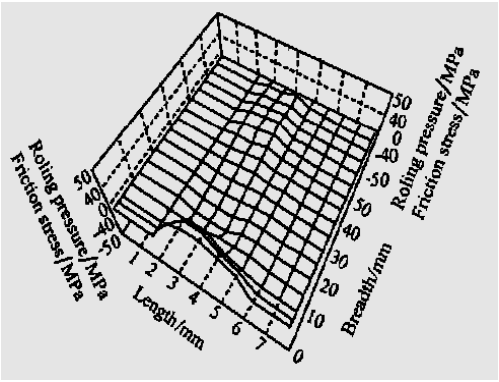

Fig 10. Friction stress distribution on the width direction.

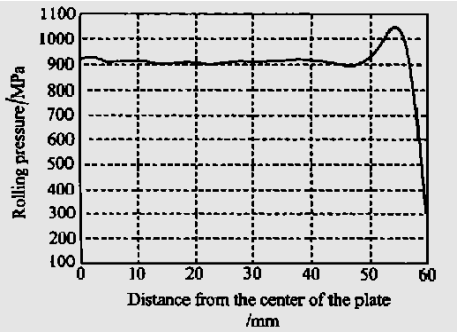

Fig 11. Fringe influence on the rolling stress.

Further, we use adaptive control technology for numerical calculation of rolling force and find out the calculated value of rolling force. Then we compare it with the result of not using adaptive control technology model, see Fig. (12). From comparative analysis we know that when not using adaptive control technology, mean square error of calculated value and measured value is $\sigma = 14.9\%$; when using adaptive control technology, mean square error is $\sigma = 8.4\%$. So our algorithm can significantly improve the setting precision of the rolling force and meet the requirements of online control.

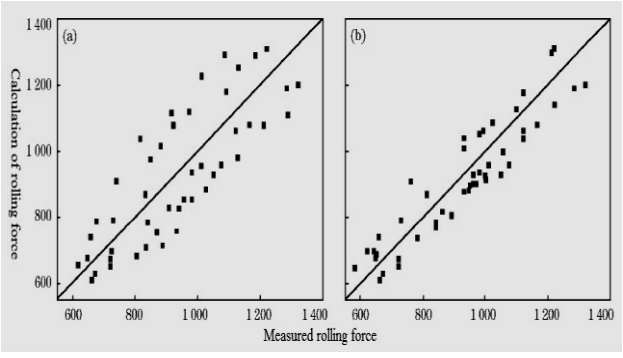

Fig 12. Comparison of rolling force calculated and measured values.

4 CONCLUSIONS

In the paper, we combine three-dimensional elastic-plastic contact BEM parallel condensed algorithm with the adaptive algorithm, then numerically simulate the setting of the rolling force. Examples prove that our algorithm obtains high parallel speedup ratio and parallel efficiency and improve the calculation accuracy and computational efficiency.

5 ACKNOWLEDGEMENTS

This research is partially supported by the National Natural Science Foundation of Hebei Province (No. E2013209215) and Tangshan Science and Technology Project (14130271a).

6 REFERENCE

►Tiantang Yu, Hongdao Jiang. Design and implementation of FEM parallel program. Journal of Numerical Methods and Computer Applications, 2000, 6(2): 155-160.

►Qingxue Huang, Hong Xiao, Guangxian Shen. BEM analysis of rolling pressure and frictional stress by measured elastic deformation. Chinese Journal of Computational Mechanics, 1998, 15(2): 49-54.

►Dexing Luo, Qian Chen, Liwen Liu. Finite element analysis for effect of roller radius on metal deformation. Iron and Steel, 2004, 39(1): 39 -43.

►Lizhong Liu, Xianghua Liu, Xudong Zhou, Guodong Wang. Simulation on the unsteady deformation of slab rolling in the bite stage. Journal of Plasticity Engineering, 2001, 8(3): 67 -70.

►Hong Xiao, Guangxian Shen, Jiachuang Lian. Simulation of strip rolling process by 3-dimensional elastoplastic boundary element method. Iron and Steel, 1993(3): 39-43.

►Hong Xiao. Boundary element method for three dimensional elastic-plastic contact problems and its application in plate rolling process. Journal of Yanshan university, 2000, 24(4): 363-368.

►Deyi Liu, Guangxian Shen, Hong Xiao. Multipole BEM for three dimensional elasto-plastic contact with friction. Journal of Yanshan university, 2004, 28(2): 99-102.

►Zhe Sun, Minhong Zhang. Elastro-plastic FEM analysis of strip steel rolling. Journal of Baotou University of Iron and Steel Technology, 2002, 21(1): 35 -37.

►Yanwen Wang, Yonglin Kang, Zhiyong Yu, Dahuan Yuan, Yuenan Chen, Guofu Wang. Three dimensional FEM simulation of square billet rolling box roll-profile. Iron and Steel, 2000, 35(2): 38 -40.

►Jiachang Sun. Network parallel computing and distributed programming environment. Beijing: Science press, 1996.

►Chenxin Liu. The Numerical Simulation of Medium Plate Rolling Deformation. Wide and Heavy Plate, 2014, 20(6): 34-39.

►Jinlan Bai, Junsheng Wang, Guodong Wang, Xianghua Liu. Improvement in Setting Accuracy of Rolling Force Model During Process Control of Cold Rolling. Journal of Iron and Steel Research, 2006, 18(3): 21-25.

►Jiangbo Dai, Qingdong Zhang, Xianlin Chen, Lin Sun, Guangxin Zhang, Chen Zhang. Development of rolling force model for 2800mm steel plate finshing mill. Journal of University of Science and Technology Beijing, 2002, 24(3): 318 -321.

►Junsheng Wang, Jinlan Bai, Xianghua Liu. Principle and process control of cold strip rolling. Beijing: Science press, 2009: 299.

►Meijuan Song, Jie Yang, Yansheng Hu. Research on online determination of gain coefficient in self-adaptive control of hot rolled strip. Research on Iron & Steel, 1996 (5): 15-18.